Aust. J. Phys., 1987, **40**, 557–86

Spectral Behaviour of Pulse Width in Pulsars

O. B. Slee,[A] *A. D. Bobra*[B] *and S. K. Alurkar*[B]

[A] Division of Radiophysics, CSIRO, P.O. Box 76,
Epping, N.S.W. 2121, Australia.
[B] Physical Research Laboratory, Ahmedabad 380 009, India.

Abstract

The profiles of 24 pulsars have been measured with the Culgoora circular array at 80 and 160 MHz. The low-frequency profile widths have been combined with most of the published higher frequency widths to generate their pulse-width spectra. We find that:

(i) pulse-width spectra follow a power law, with indices ranging between $+0\cdot09$ and $-0\cdot60$ and a median of $\beta = -0\cdot16$;

(ii) the spectrum of the spacings between the outer components of multiple profiles has the same slope as that of the total width at $\nu < 1$ GHz but flattens significantly at higher frequencies;

(iii) there is a significant relationship between pulse-width spectra and flux spectra—steep flux spectra are associated with flat width spectra;

(iv) the large dispersion in width-spectrum slopes suggests that there are large departures from the simple dipole magnetic field usually assumed in models for pulsar emission.

1. Introduction

Surprisingly, very little systematic study has hitherto been made of the widths of averaged pulsar profiles as a function of frequency. More attention seems to have been paid to the spectral variation in the spacings between components of double and triple profiles—see e.g. Craft and Comella (1968), Komesaroff *et al.* (1970), Lyne *et al.* (1971) and Sieber *et al.* (1975), who showed that generally the spacings between components decreased continuously with increasing frequency, although the variation was usually more complex than a simple power law.

The only more general investigations of other morphological species of profiles previously made have been by Backer (1976), Rankin (1983) and (of one particular pulsar, 0809+74) Bartel *et al.* (1981). These authors found that the full width to half-power had often a basic power-law variation with frequency, in the sense that, like the spacings between components of multiple profiles, the width decreased with frequency. The power-law index did however vary between zero and $-0\cdot33$.

The underlying power-law variation in pulse width seems understandable in terms of the polar cap emission model, where the cone of emission would contain the higher frequency emitting regions nearer its apex than the regions emitting the lower frequencies. If we postulate that the double profiles are due to the observer's line of sight sweeping across the centre of a hollow cone of emission, then the fact that the

0004-9506/87/040557$02.00

widths of the individual components and their spacing both decrease with frequency is also understandable.

The present study was prompted by low-frequency pulsar measurements at 80 and 160 MHz with the Culgoora circular array. The data, taken during 18 months in 1979/80, have already been utilised to investigate the metre-wave flux densities, spectra and variability of pulsars (Slee *et al.* 1986) and in a study of interstellar scattering (Alurkar *et al.* 1986). Since these observations are probably the most comprehensive and systematic hitherto conducted on a large number of pulsars at low frequencies, their inclusion in a study of pulse-width behaviour is well justified.

The Culgoora low-frequency measurements of pulse width and component separation for the multiple profiles are presented in Section 2. In Section 3 these measurements are combined with most other published pulse widths and separations at higher frequencies to generate the pulse-width spectra. Section 4 examines the relationships between the pulse-width spectral index β and the intrinsic pulsar parameters. We discuss the implications of our findings in Section 5.

2. Culgoora Measurements of Pulse Width

The reader is referred to Slee *et al.* (1986) and Alurkar *et al.* (1986) for details of the pulsar observing procedure and subsequent analysis. In this investigation we attempt to determine the intrinsic pulse widths from the observed averaged profiles. For the single profiles we convolved a gaussian pulse with functions representing the dispersion bandwidth smearing and the RC integration time constant. Least-squares fitting of the convolved pulse with the observed profile was then performed, with the intrinsic pulse width as the adjustable parameter. For the multiple profiles the total width between the external half-power points on the outer components was manually measured and a small approximate correction made for dispersion smearing and time constant. The spacing between the centres of the outer components was also measured. Fig. 1 shows typical 80 and 160 MHz pulse profiles for the pulsars that were included in computations of pulse-width spectra.

Some authors, notably Rankin (1983), have measured the outer half-power point on each component separately and then defined the half-power width of the multiple profile as the interval between these points. We have preferred to locate the outer points at the half-power levels of the highest amplitude component; we consider this to be more consistent with the method of measuring the widths of apparently single profiles, which in most cases probably contain unresolved components. However, our method does lead to a discontinuity in the pulse-width spectrum if the height of one pulse falls below half that of the other. An example of this is shown in the spectrum of 1133+16 in Fig. 2*i*.

The 80 and 160 MHz pulse widths to half-power points W_{50} are tabulated in Table 1 for all the pulsars with an adequate signal to noise ratio and no evidence

---

Figs 1*a*–1*n*. Typical pulse profiles for the pulsars included in our study. In most cases the 80 and 160 MHz profiles of each pulsar were recorded quasi-simultaneously, with about thirty 60 s integrations at one frequency being interleaved with the same number of integrations at the other. Simultaneous profiles with 90 and 10 kHz bandwidths were made, but we give the less noisy 90 kHz profile unless it is important to show the pulse structure or the widening by bandwidth dispersion is excessive. The 10 kHz profiles were sampled at 3·9 ms intervals and the 90 kHz profiles at 7·8 ms intervals. The RC time constants of the integrators were 4 and 8 ms for the 10 and 90 kHz bandwidths respectively. Baselines are least squares fits to the data.

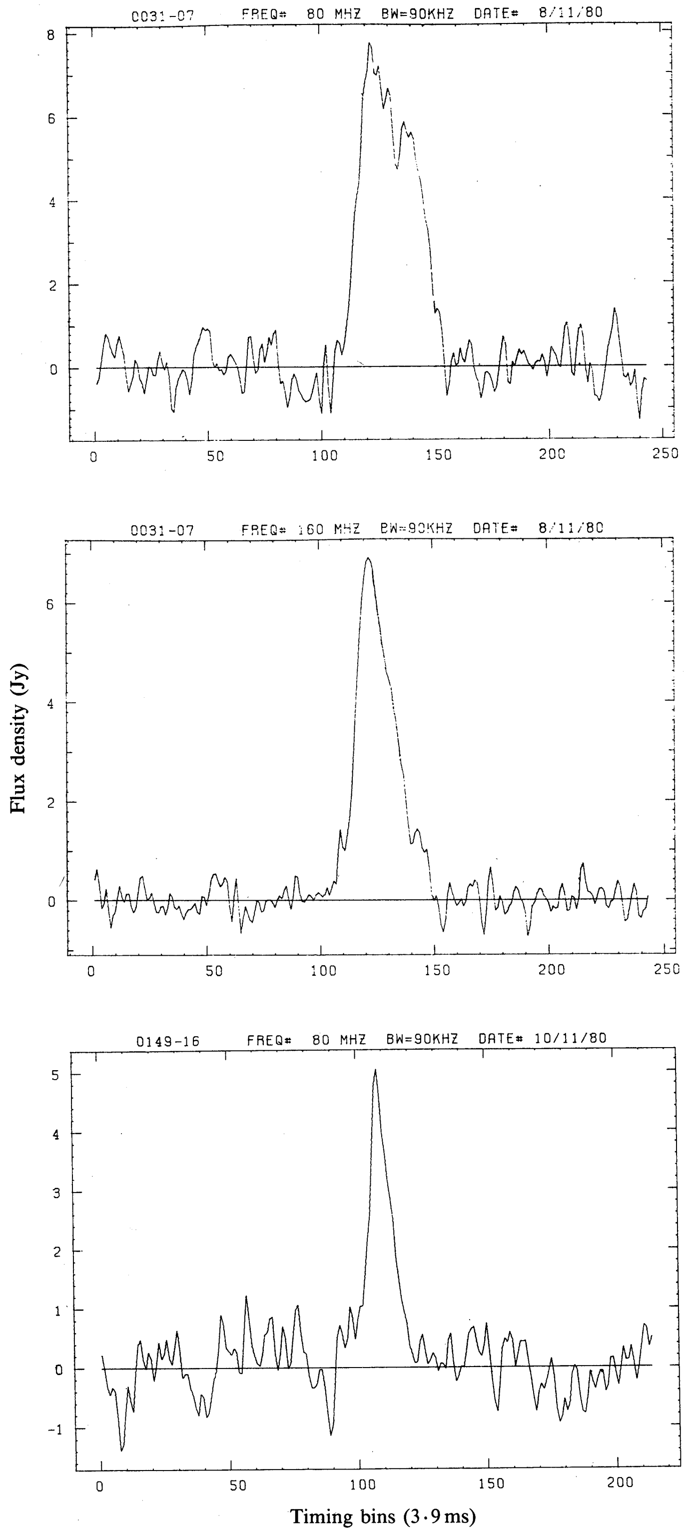
0031-07 FREQ= 80 MHZ BW=90KHZ DATE= 8/11/80
0031-07 FREQ= 160 MHZ BW=90KHZ DATE= 8/11/80
0149-16 FREQ= 80 MHZ BW=90KHZ DATE= 10/11/80
Flux density (Jy)
Timing bins (3·9 ms)

Fig. 1*a*

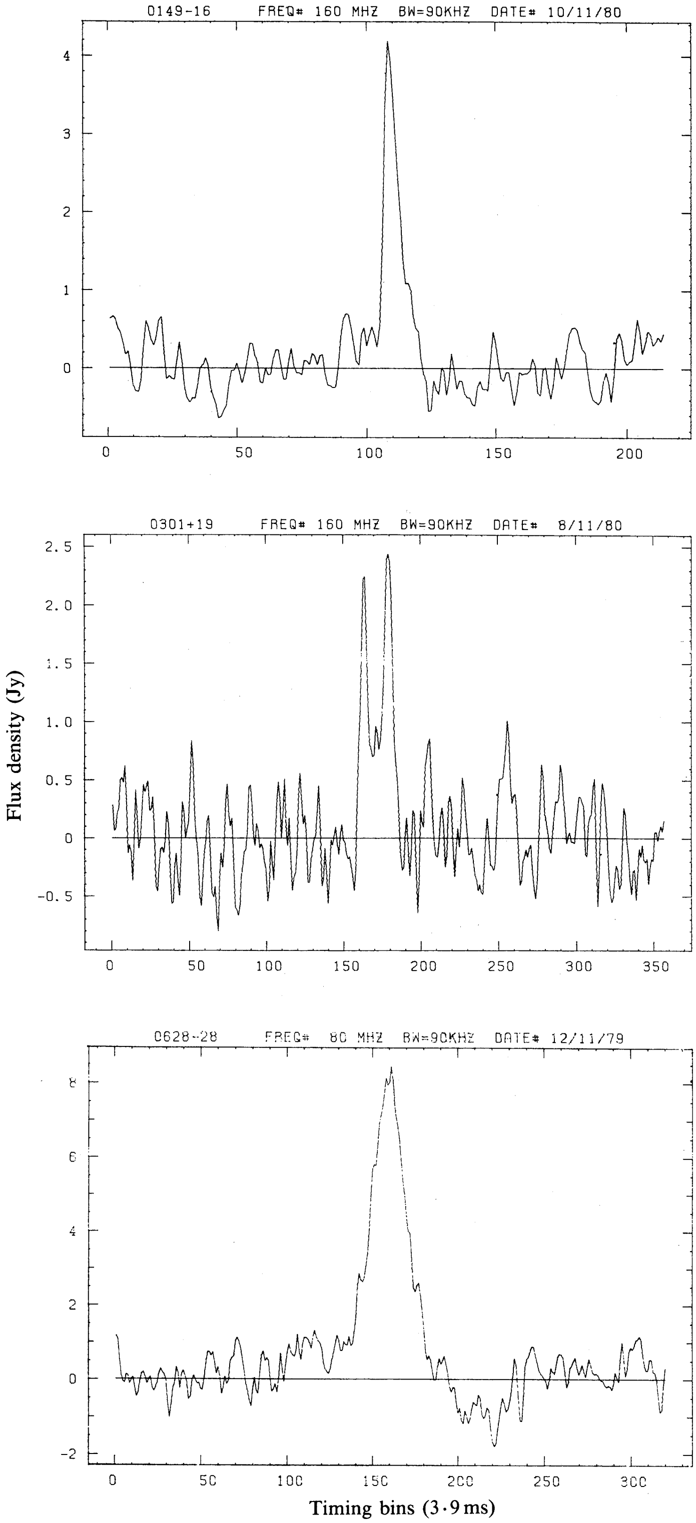
0149-16 FREQ= 160 MHZ BW=90KHZ DATE= 10/11/80
0301+19 FREQ= 160 MHZ BW=90KHZ DATE= 8/11/80
0628-28 FREQ= 80 MHZ BW=90KHZ DATE= 12/11/79
Flux density (Jy)
Timing bins (3·9 ms)

Fig. 1*b*

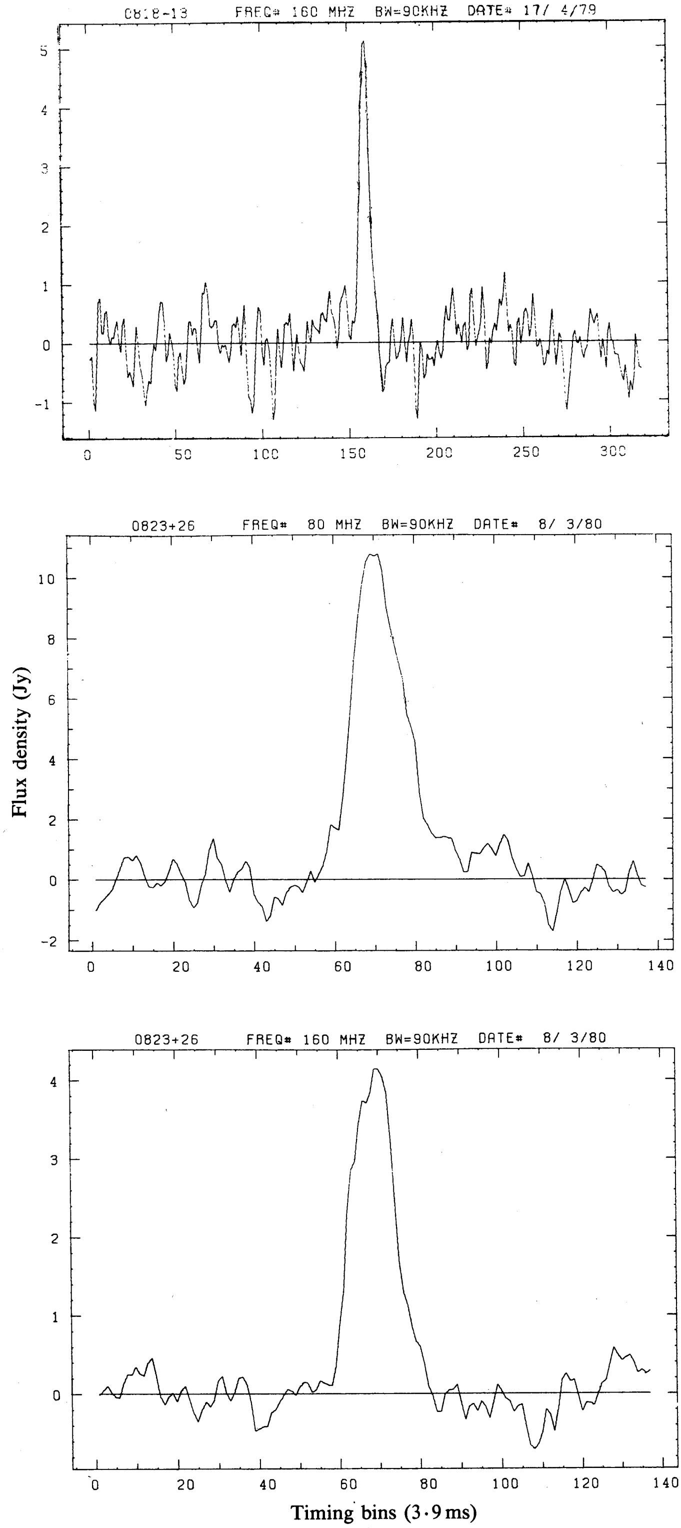
0818-13 FREQ= 160 MHZ BW=90KHZ DATE= 17/ 4/79
0823+26 FREQ= 80 MHZ BW=90KHZ DATE= 8/ 3/80
0823+26 FREQ= 160 MHZ BW=90KHZ DATE= 8/ 3/80
Flux density (Jy)
Timing bins (3·9 ms)

Fig. 1*c*

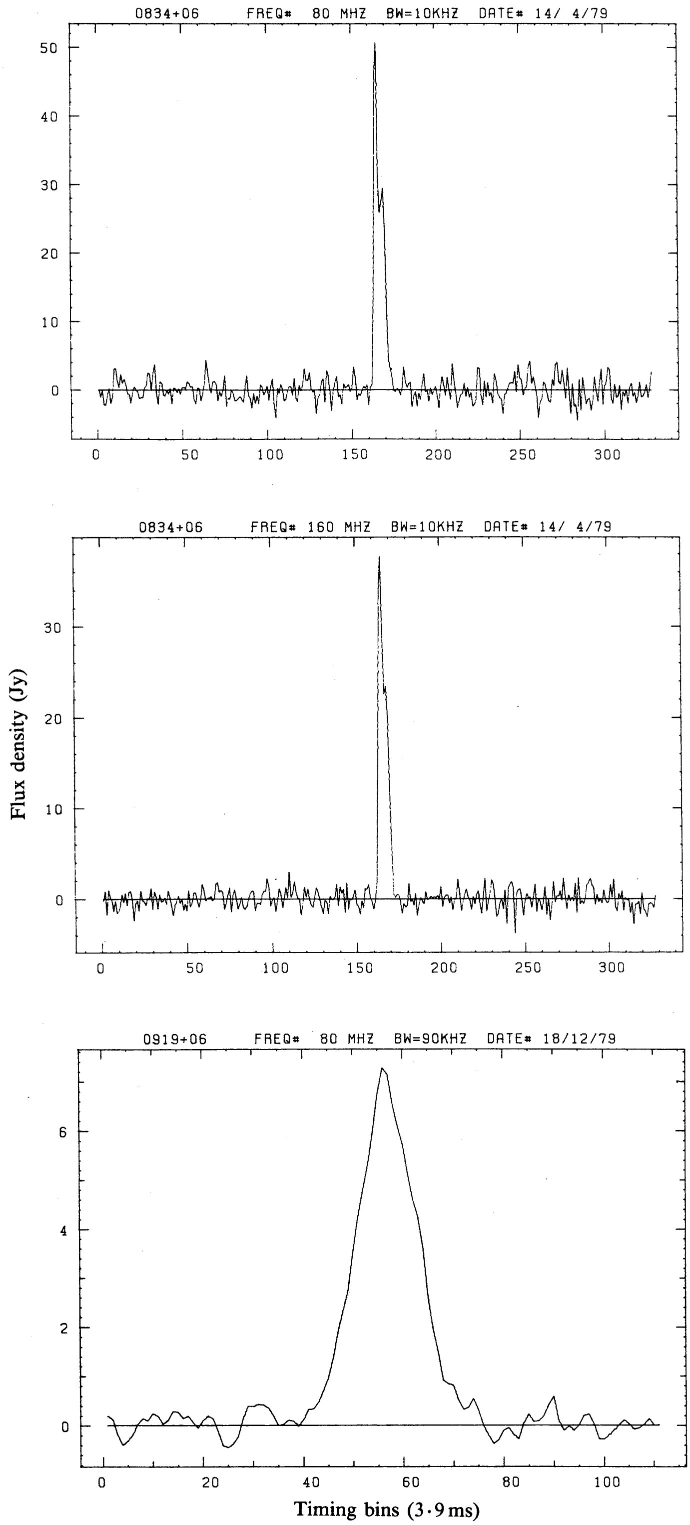
0834+06 FREQ= 80 MHZ BW=10KHZ DATE= 14/ 4/79
0834+06 FREQ= 160 MHZ BW=10KHZ DATE= 14/ 4/79
0919+06 FREQ= 80 MHZ BW=90KHZ DATE= 18/12/79
Flux density (Jy)
Timing bins (3·9 ms)

Fig. 1*d*

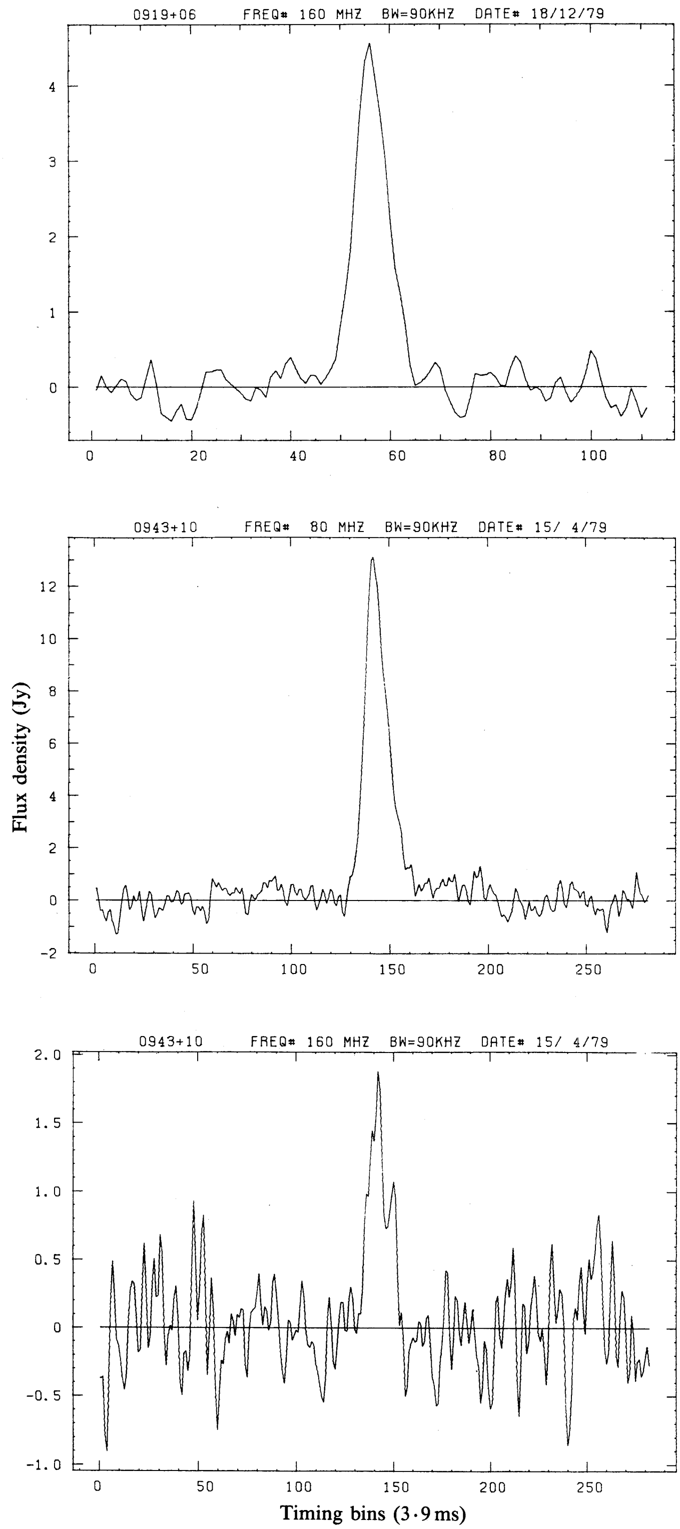
0919+06 FREQ= 160 MHZ BW=90KHZ DATE= 18/12/79
0943+10 FREQ= 80 MHZ BW=90KHZ DATE= 15/ 4/79
0943+10 FREQ= 160 MHZ BW=90KHZ DATE= 15/ 4/79
Flux density (Jy)
Timing bins (3·9 ms)

Fig. 1*e*

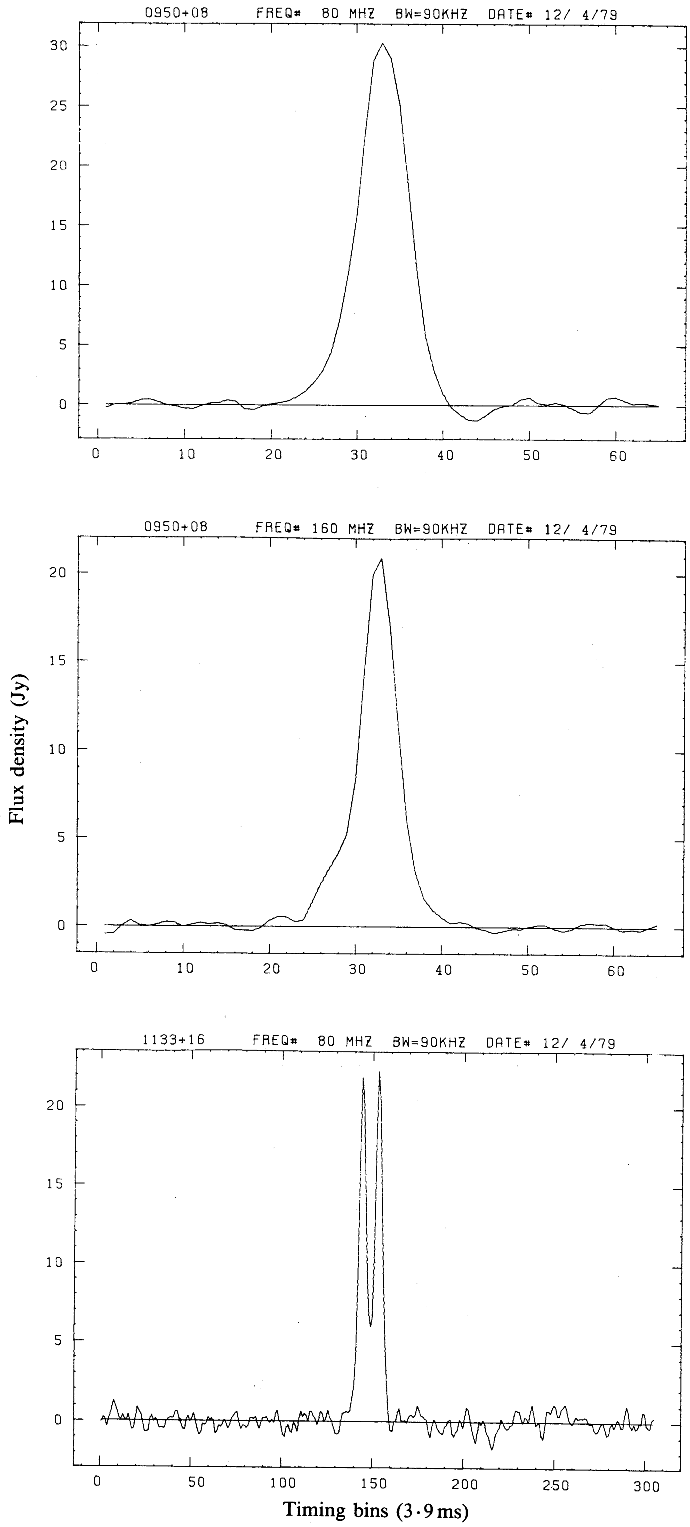
0950+08 FREQ= 80 MHZ BW=90KHZ DATE= 12/ 4/79
0950+08 FREQ= 160 MHZ BW=90KHZ DATE= 12/ 4/79
1133+16 FREQ= 80 MHZ BW=90KHZ DATE= 12/ 4/79
Flux density (Jy)
Timing bins (3·9 ms)

Fig. 1*f*

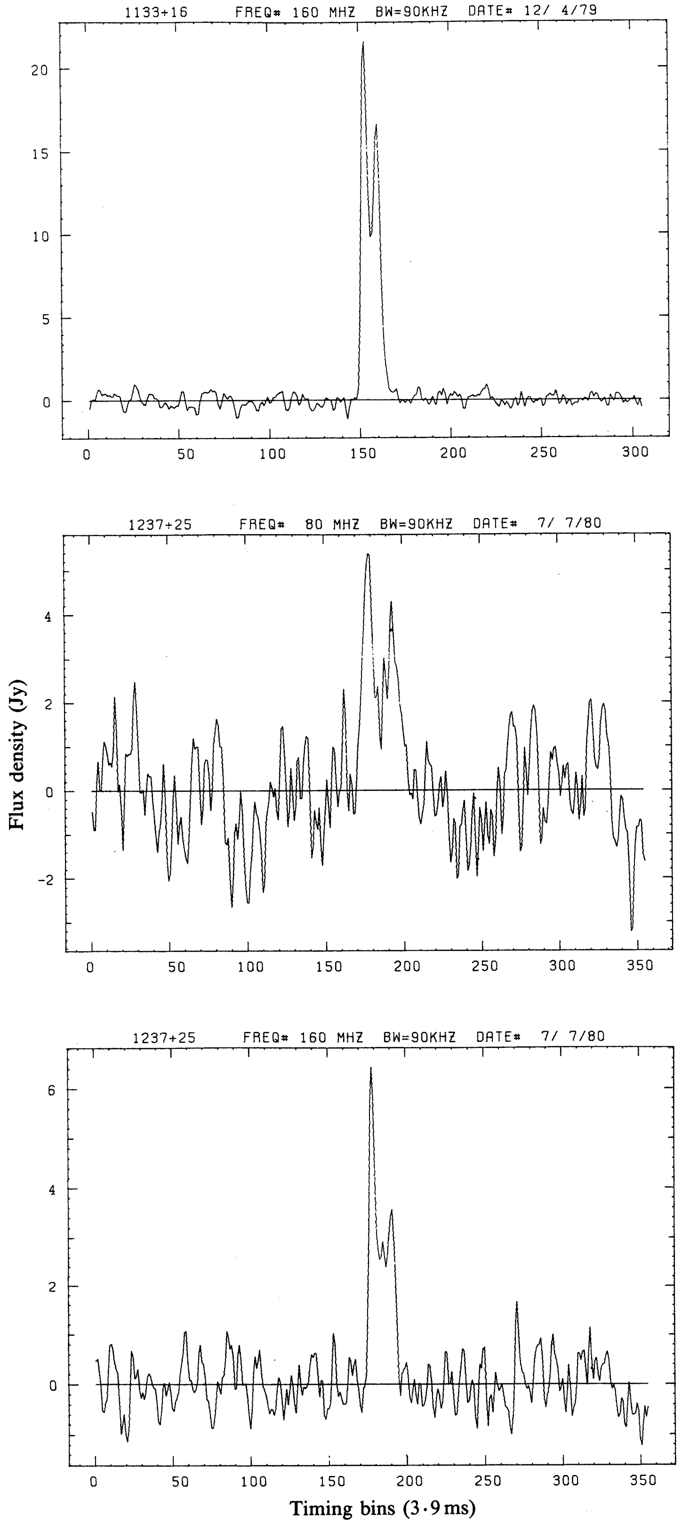
1133+16 FREQ= 160 MHZ BW=90KHZ DATE= 12/ 4/79
1237+25 FREQ= 80 MHZ BW=90KHZ DATE= 7/ 7/80
1237+25 FREQ= 160 MHZ BW=90KHZ DATE= 7/ 7/80
Flux density (Jy)
Timing bins (3·9 ms)

Fig. 1*g*

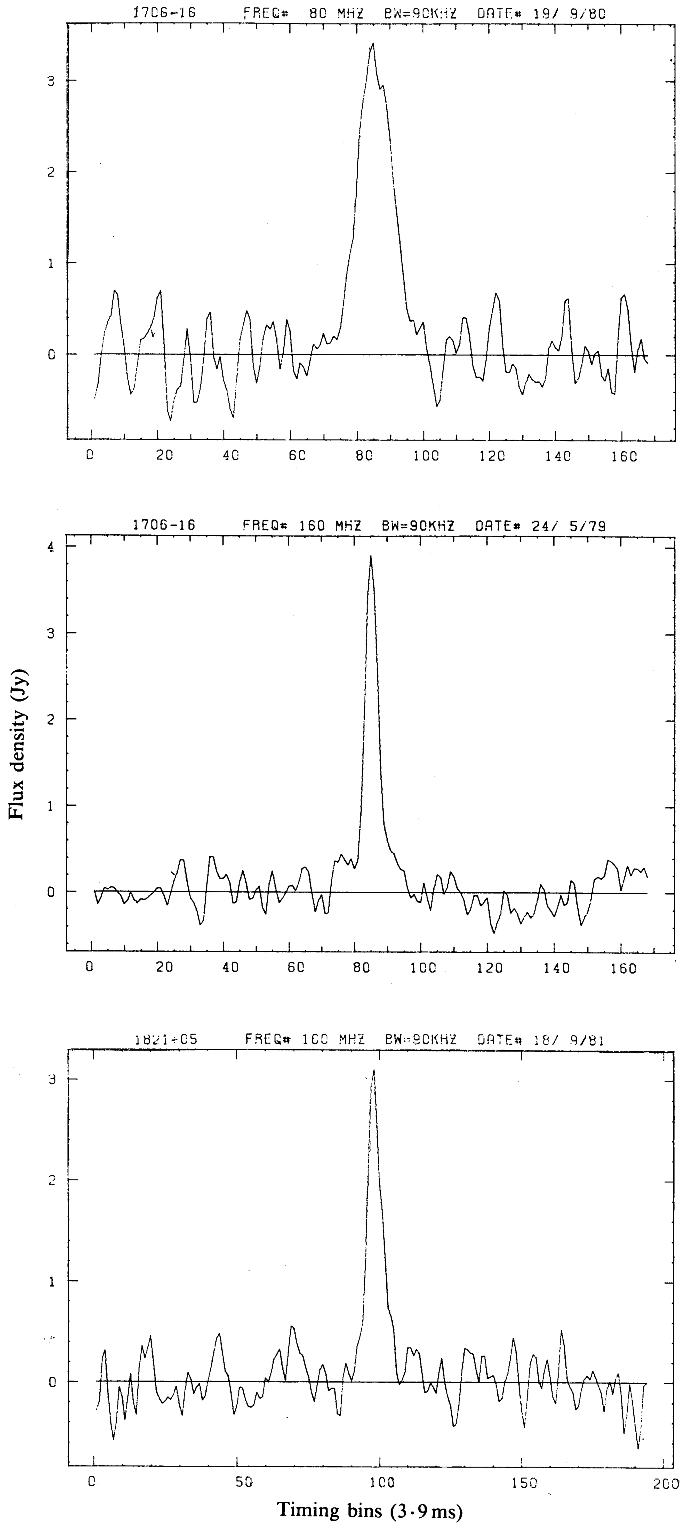
1706-16 FREQ= 80 MHZ BW=90KHZ DATE= 19/ 9/80
1706-16 FREQ= 160 MHZ BW=90KHZ DATE= 24/ 5/79
1821+05 FREQ= 100 MHZ BW=90KHZ DATE= 18/ 9/81
Flux density (Jy)
Timing bins (3·9 ms)

Fig. 1*j*

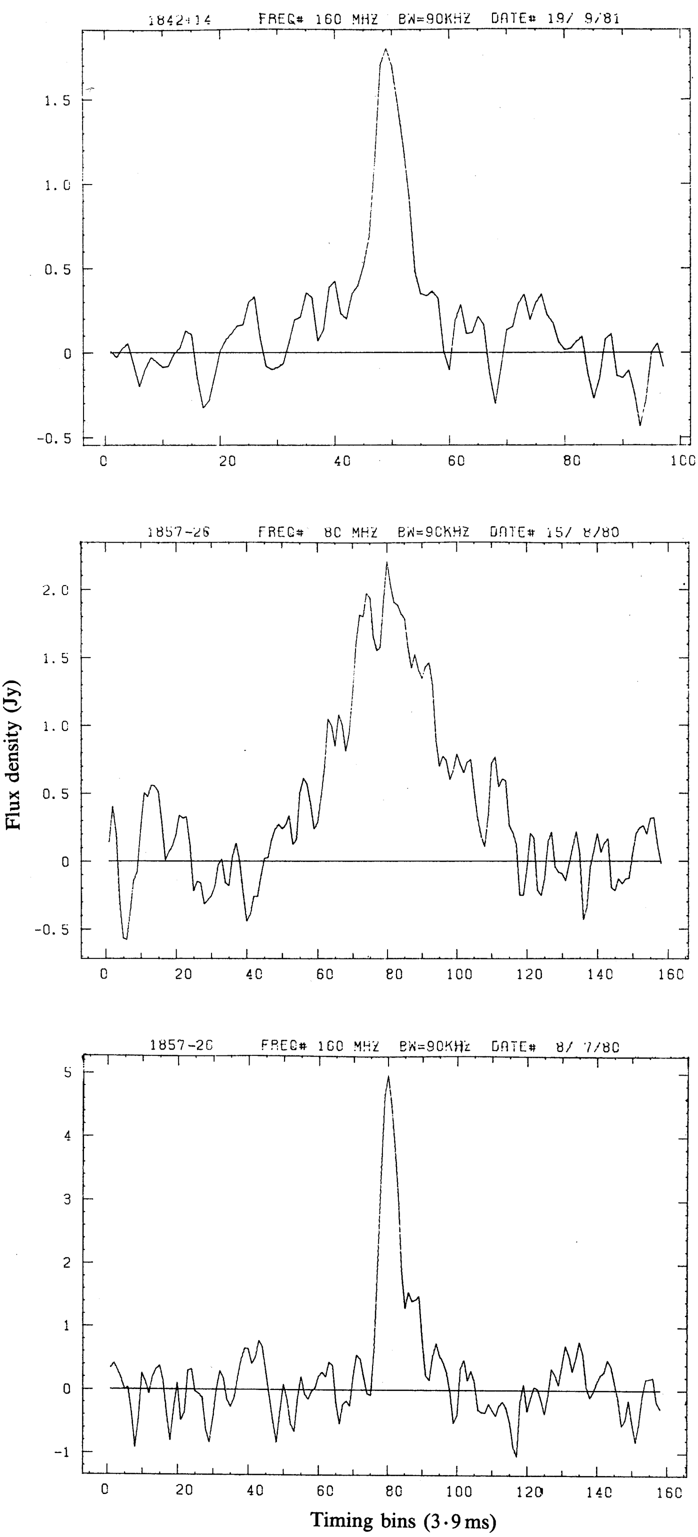
1842+14 FREQ# 160 MHZ BW=90KHZ DATE# 19/ 9/81
1857-26 FREQ# 80 MHZ BW=90KHZ DATE# 15/ 8/80
1857-26 FREQ# 160 MHZ BW=90KHZ DATE# 8/ 7/80
Flux density (Jy)
Timing bins (3·9 ms)

Fig. 1*k*

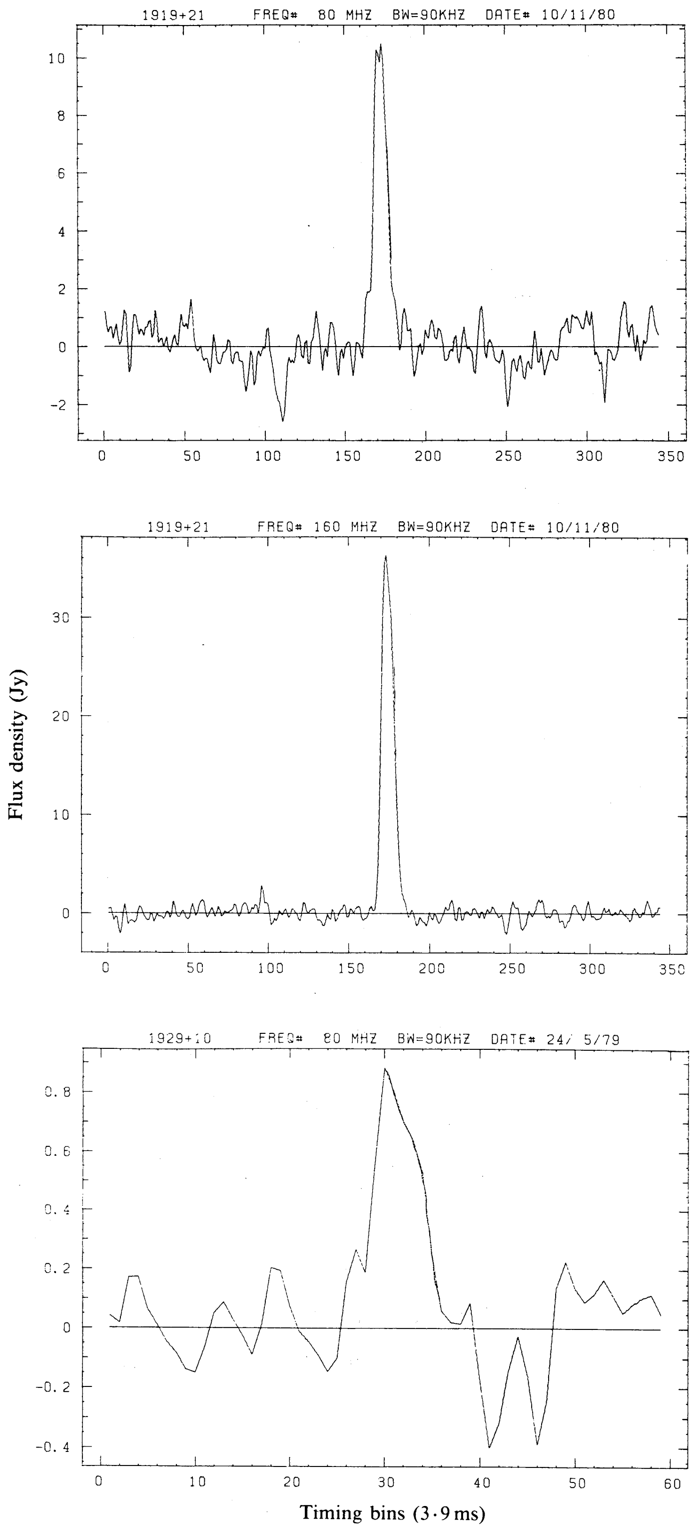
1919+21 FREQ= 80 MHZ BW=90KHZ DATE= 10/11/80
1919+21 FREQ= 160 MHZ BW=90KHZ DATE= 10/11/80
1929+10 FREQ= 80 MHZ BW=90KHZ DATE= 24/ 5/79
Flux density (Jy)
Timing bins (3·9 ms)

Fig. 1*l*

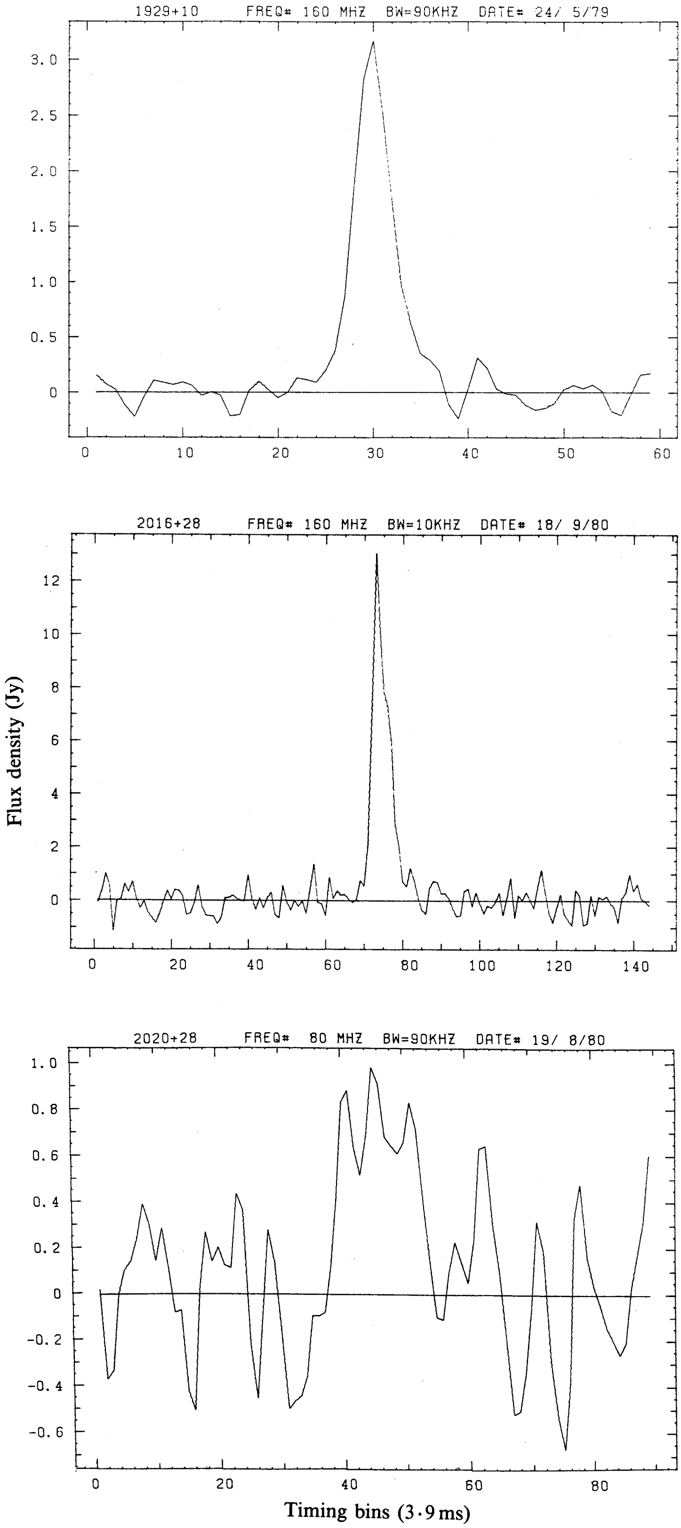
1929+10 FREQ= 160 MHZ BW=90KHZ DATE= 24/ 5/79
3.0
2.5
2.0
1.5
1.0
0.5
0
0 10 20 30 40 50 60
2016+28 FREQ= 160 MHZ BW=10KHZ DATE= 18/ 9/80
12
10
8
6
4
2
0
0 20 40 60 80 100 120 140
Flux density (Jy)
2020+28 FREQ= 80 MHZ BW=90KHZ DATE= 19/ 8/80
1.0
0.8
0.6
0.4
0.2
0
-0.2
-0.4
-0.6
0 20 40 60 80
Timing bins (3·9 ms)

Fig. 1*m*

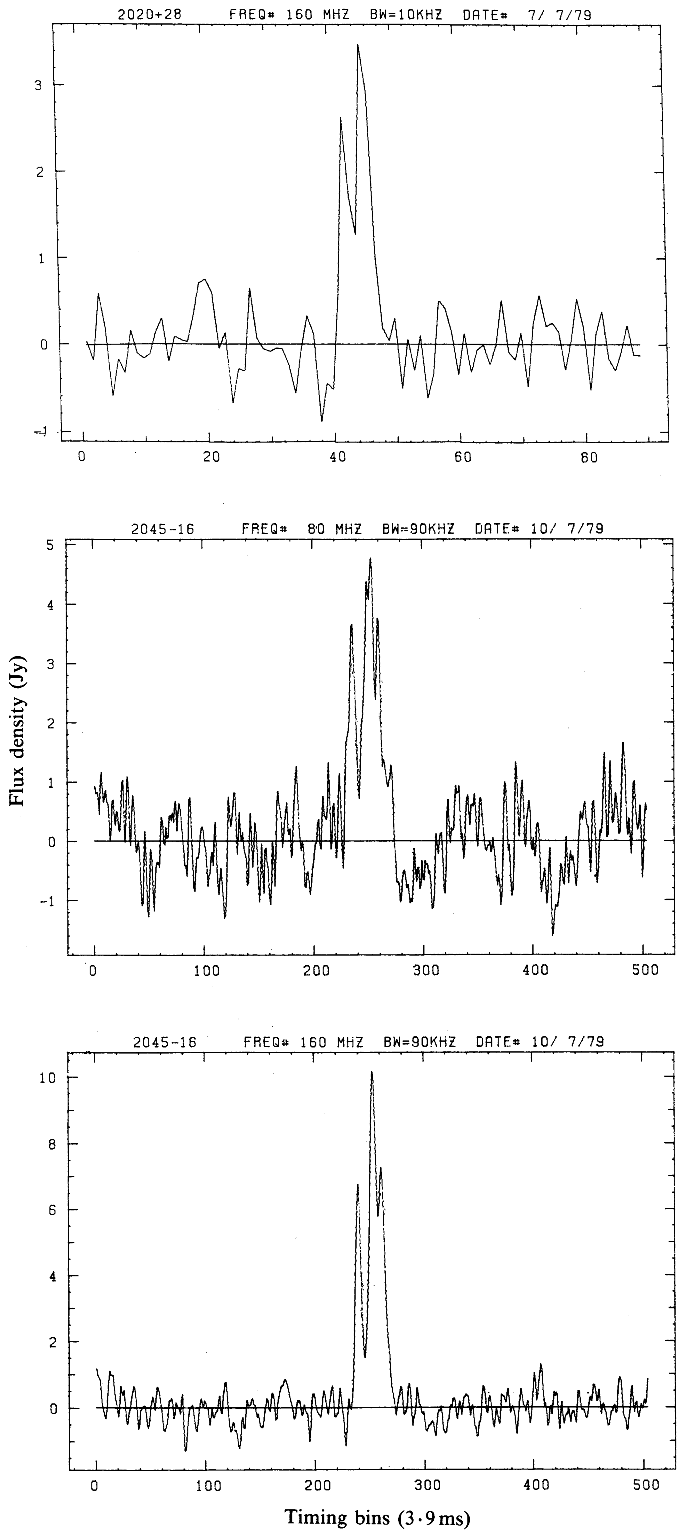
2020+28 FREQ= 160 MHZ BW=10KHZ DATE= 7/ 7/79
2045-16 FREQ= 80 MHZ BW=90KHZ DATE= 10/ 7/79
Flux density (Jy)
2045-16 FREQ= 160 MHZ BW=90KHZ DATE= 10/ 7/79
Timing bins (3·9 ms)

Fig. 1*n*

for pulse widening due to interstellar scattering. When four or more independent measurements were made the standard errors quoted are estimated from the scatter about the means. When less than four profiles were available the r.m.s. scatter about the fitted baselines was used to provide an error estimate via a regression equation between that quantity and the percentage standard deviation in pulse width for the well-observed pulsars.

Table 1. Pulse widths and component separations (in degrees)

Pulsar	160 MHz			80 MHz		
	No. obs.	3 dB pulse width (W_{50})	Outer component spacing	No. obs.	3 dB pulse width (W_{50})	Outer component spacing
0031−07	4	25·7±1·1		4	40·2±2·2	
0149−16	4	7·69±0·99		4	9·4±2·5	
0301+19	1	21·8±0·8	16·0±0·9			
0628−28				3	20·5±1·7	
0818−13	6	5·96±0·93				
0823+26	1	6·1±2·2		1	5·4±1·9	
0834+06	4	5·60±0·08	3·48±0·62	4	6·70±0·25	4·92±0·40
0919+06	9	21·4±0·6		8	23·5±0·8	
0943+10	3	14·2±2·5		9	13·2±0·8	
0950+08	6	21·1±1·1		8	31·2±1·0	14·1±1·6
1133+16	8	12·7±0·2	8·55±0·15	8	15·1±0·2	10·7±0·2
1237+25	10	16·1±0·8	12·8±0·3	3	16·8±1·1	15·9±1·1
1541+09	8	25·8±3·4		8	28·1±2·0	
1604−00	7	11·9±0·5		4	17·0±2·0	
1642−03	5	4·17±0·46		4	4·74±0·56	
1706−16	4	7·50±0·33		8	11·7±0·9	
1821+05	1	6·69±0·76				
1842+14	1	20·2±3·0				
1857−26	4[A]	11·3±1·7		6	41·6±6·4	
1919+21	6	7·27±0·11		4	6·81±0·40	
1929+10	2	19·3±1·0		2	27·7±5·4	
2016+28	2	12·2±0·6				
2020+28	3	22·0±2·2	14·3±0·8	1	17·8±6·9	
2045−16	6	18·1±0·7	15·0±0·2	3	21·3±0·8	17·9±0·7

[A] Measurement refers to the major component of the profile.

3. Pulse-width Spectra

We have combined our 80 and 160 MHz estimates of pulse width with most other published values to obtain pulse-width spectra up to 10·7 GHz. In most cases we were obliged to measure the half-power widths from published small-scale profiles and so the accuracies of individual measurements are not high. However, many points on the spectra are averages of up to eight independent measurements by different groups

Figs 2*a*–2*q* (see over). Spectra of profile widths for the well-observed pulsars. Here W is the full half-power width of the profile in units of degrees of rotation, and C is the component separation for those pulsars with double profiles or between the centres of the outer components of PSR 2045−16. The dashed lines are the power-law regression lines for the W points and their slopes are given in Table 3. Points without error bars possess errors less than or equal to the dot diameter.

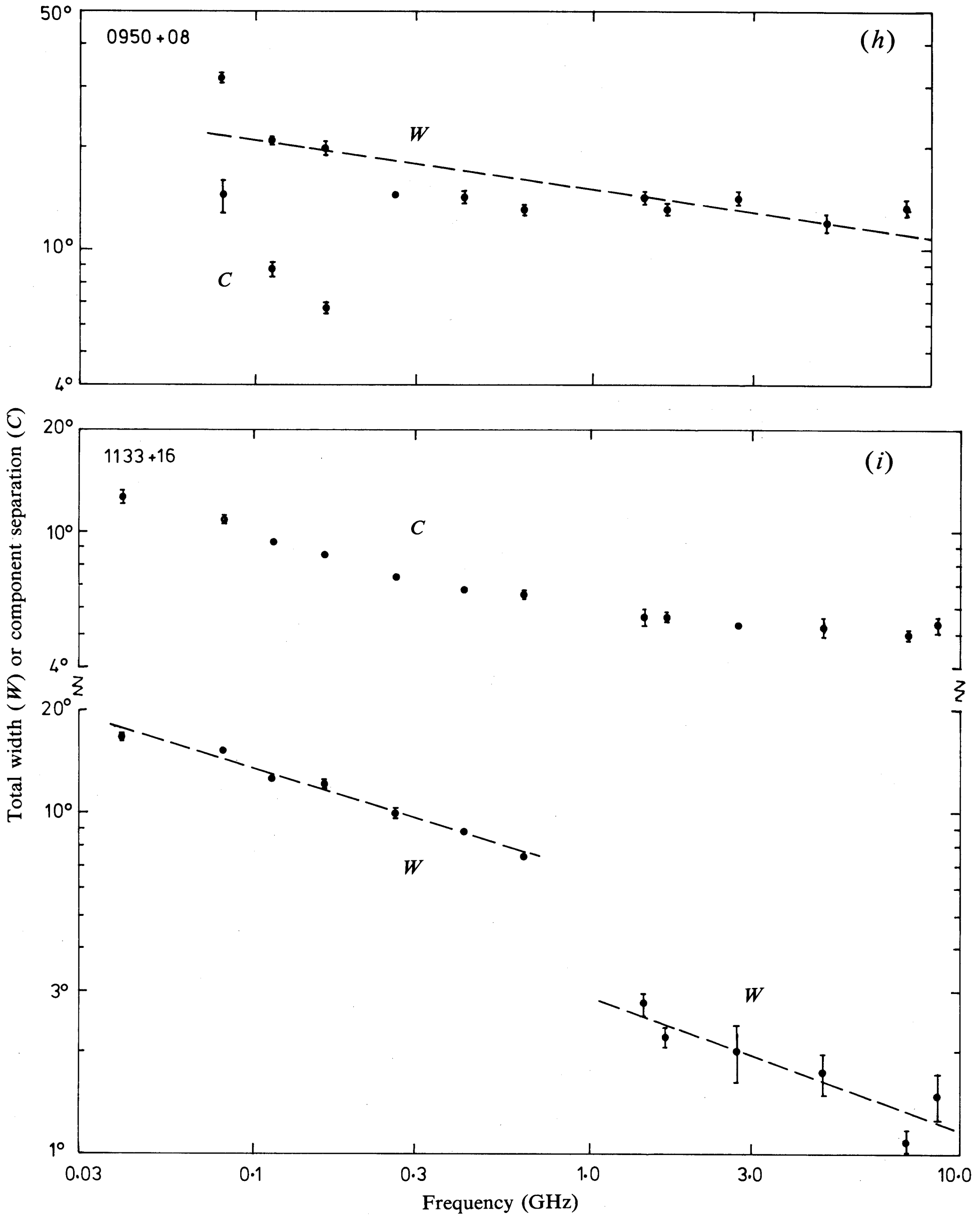

Figs 2*h* and 2*i*

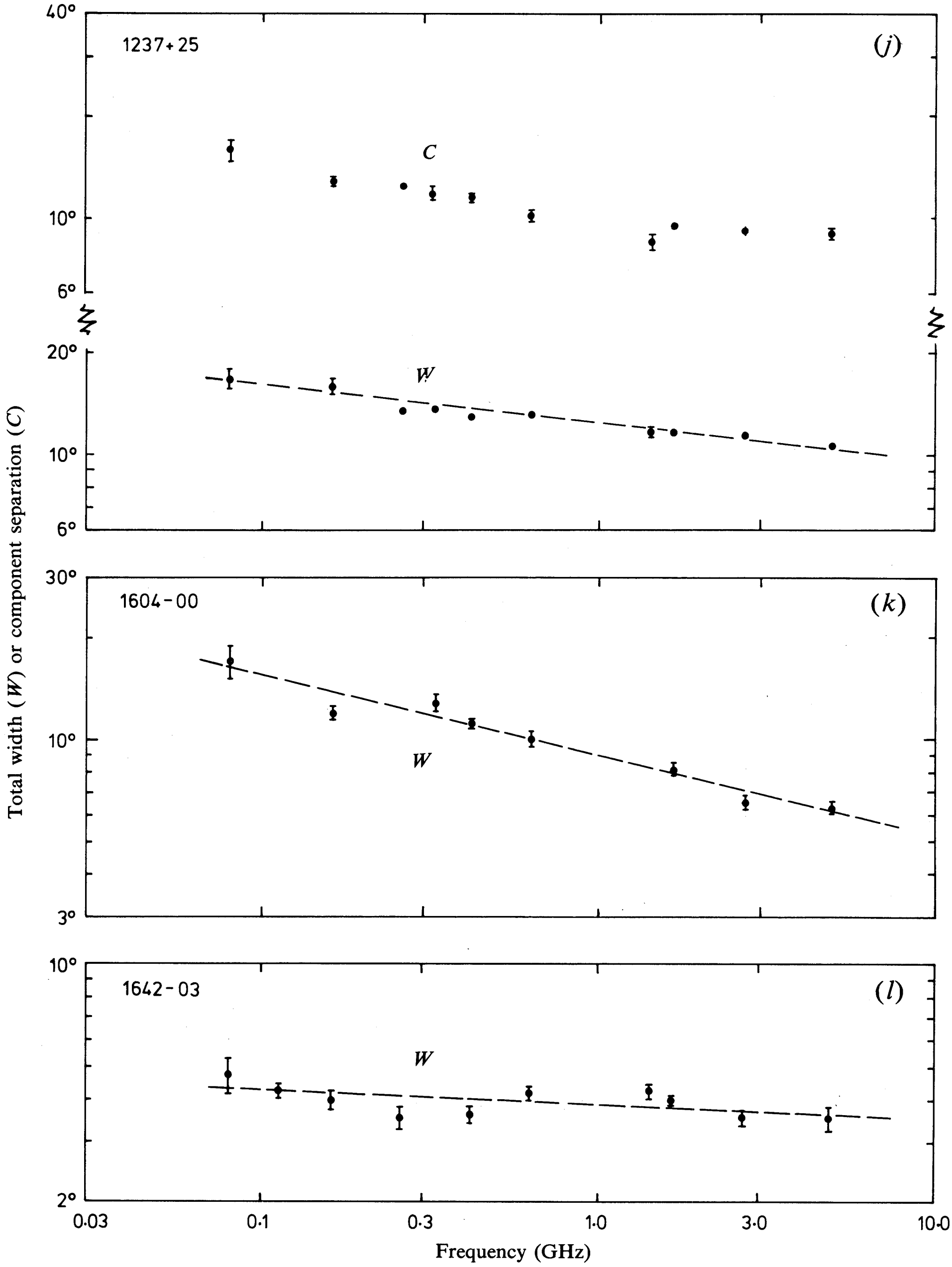
1237+25
(j)
C
W
40°
10°
6°
20°
10°
6°
1604-00
(k)
W
30°
10°
3°
1642-03
(l)
W
10°
2°
Total width (W) or component separation (C)
0.03
0.1
0.3
1.0
3.0
10.0
Frequency (GHz)

Figs 2j–2l

Table 2. Data sets for averaged pulse profiles

Frequency band (GHz)	References to pulse profiles
0·040	Craft and Comella (1968)
0·080	Present paper
0·111 to 0·113	Craft and Comella (1968); Manchester (unpublished)
0·150 to 0·170	Komesaroff *et al.* (1970); Lyne *et al.* (1971); Schwarz and Morris (1971); Present paper; Manchester (unpublished)
0·230 to 0·281	Craft and Comella (1968); Lyne *et al.* (1971); Manchester (unpublished)
0·318 to 0·327	Backer (1970); Krishna Mohan *et al.* (1971)
0·400 to 0·430	Ashworth and Lyne (1981); Backer *et al.* (1973); Craft and Comella (1968); Hamilton *et al.* (1977); Komesaroff *et al.* (1970); Lyne *et al.* (1971); Manchester (1971, 1975, and unpublished); Rankin (1983); Rankin and Benson (1981); Schönhardt and Sieber (1973)
0·610 to 0·640	Ashworth and Lyne (1981); Lyne *et al.* (1971); Manchester (unpublished); McCulloch *et al.* (1978)
1·400 to 1·420	Backer (1972); Lyne and Hamilton (unpublished); Sieber and Wielebinski (1973)
1·612 to 1·720	Komesaroff *et al.* (1970); Manchester (1971); Manchester *et al.* (1980); Morris *et al.* (1981)
2·650 to 2·700	Komesaroff *et al.* (1970); Morris *et al.* (1970, 1981); Sieber *et al.* (1975)
4·850 to 5·000	Backer (1972); Crovisier (1973); Sieber *et al.* (1975)
8·70	Morris *et al.* (1981)
10·70	Sieber *et al.* (1975)

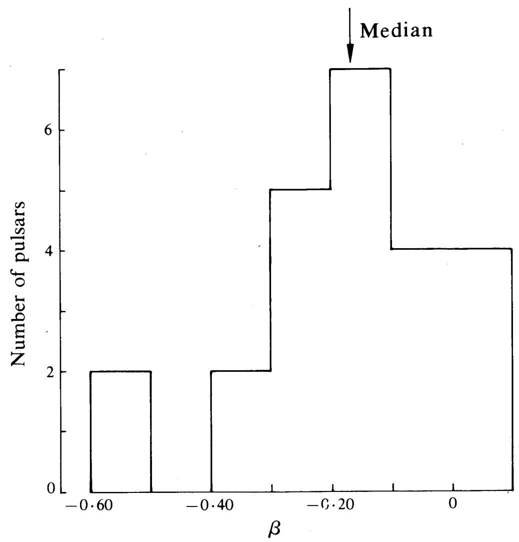

Fig. 3. Distribution of the pulse-width spectral index β. The median is $\beta = -0\cdot16$.

and so the errors have been reduced to acceptable proportions. The data used in these computations are identified in Table 2.

Fig. 2 shows samples of the derived pulse-width spectra for the well-observed pulsars. The error bars on each point have a total length of 2σ and have been derived by two methods: (i) the averages formed from ⩾4 independent measurements have error bars equal to their standard errors; (ii) errors for the averages of <4 independent measurements have been estimated to the accuracy to which it was possible to measure the half-power widths with a ruler.

It is clear from Fig. 2 that the width spectra are approximately power-law form and possess a fairly wide range of slopes. The steepest spectrum is that for 0919+06, with a slope of −0·60, but most pulsars possess much flatter spectra, the median value for the power-law index being −0·16 (26 pulsars). The distribution of pulse-width spectral indices shown in Fig. 3 is not highly peaked and is markedly asymmetrical with a tendency to favour flatter spectra. There are two pulsars in the sample (0834+06 and 1919+21) with significantly positive spectral slopes, a property, which to our knowledge, has not been hitherto reported. The spectral indices derived from the least-squares power fits are given in Table 3.

We also show in Fig. 2 plots of the spacing between the outer components of well-resolved multiple profiles. These spectra have in general similar slopes to those of the half-power widths, with the notable difference in four of the five pulsars that the spectrum flattens significantly at the high-frequency end. This was first noticed in 1133+16 by Craft and Comella (1968) and the present measurements suggest that this is a fairly general property. Despite the existence of this effect we have fitted simple power laws to all the points, and their indices are also listed in Table 3.

Another feature in some of the spectra is the presence of one or two low points which fall significantly below the power-law regression line of best fit. Similar effects have been reported by Bartel *et al.* (1981) in the low-frequency pulse-width spectrum of 0809+74 and by Rankin (1983) in several other pulsars. It is not clear that these are real; for example, Rankin found a significant dip in the low-frequency width spectrum of 0628−28 but our plot in Fig. 2*c* does not show the effect. In most of our cases there is only a single outlying point on the spectrum, and we are inclined to ascribe the discrepancy to underestimation of measurement errors or perhaps to mode changes. There may be more substance to the dip in 0950+08 (Fig. 2*h*), which has three consecutive low points on the spectrum.

4. Spectral Indices and Pulsar Parameters

The power-law indices of Table 3 (from the fitted power-law relationship $W_{50} \propto \nu^{\beta}$) have been compared with the published pulsar parameters. Most of these were taken from Manchester and Taylor (1981). Relationships were sought by making scatter plots and fitting linear regression equations.

We found no significant relationships between β and the following: the period P; the period derivative $\dot{P}$; the radio luminosity L; the derived magnetic field B_0; the timing age τ; and the duty cycle W_{50}/P. A significant correlation (95% confidence level) was found between β and the rate of loss of kinetic energy $\dot{E} = I\Omega\dot{\Omega}$, where I is the moment of inertia of the neutron star. The regression equation, $\beta = -0{\cdot}13-(5{\cdot}60\times10^{-35})\dot{E}$, with a correlation coefficient $r = -0{\cdot}52$, was derived from 24 pulsars. Caution must be exercised in accepting the validity of the correlation (since there is a large scatter about the regression line), and much of its significance relies on the two pulsars with the steepest width spectra. If one accepts the relationship then one must consider how the increasing rate of loss of rotational energy steepens the width spectrum.

between 0·40 and 10·7 GHz; data taken at different times and with a variety of bandwidths at each frequency should average out most of the effects of interstellar scintillation and intrinsic flux changes. As a check we formed a subset of $\alpha^{\dagger}_{0\cdot 40}$ from the nine pulsars in our list which had been observed simultaneously at two or three frequencies between 0·383 and 8·085 GHz by Backer and Fisher (1974) and Kuzmin *et al.* (1978). The data sets used in these computations are identified in Table 4. The flux spectral indices that we derived from all published measurements are listed in Table 3. Fig. 4 is a scatter plot of the pulse-width spectral index β against the flux spectral index $\alpha^{\dagger}_{0\cdot 40}$. The best fitting regression line has a slope of $-0\cdot 22\pm 0\cdot 06$ and the correlation coefficient for the 20 pulsars for which we have $\alpha^{\dagger}_{0\cdot 40}$ is $r = -0\cdot 67$ (significant at the 99·9% confidence level). The subset of nine pulsars which had been observed simultaneously at two or three high frequencies yielded a slope for their regression line of $-0\cdot 17\pm 0\cdot 06$ and correlation coefficient $r = -0\cdot 76$ (significant at the 98% confidence level). The $\alpha^{1\cdot 4}_{0\cdot 4}$ values derived from the 15 pulsars in our list for which Manchester and Taylor (1981) gave fluxes yield a regression line with a slope of $-0\cdot 14\pm 0\cdot 04$ and $r = -0\cdot 74$ (significant at the 99·8% confidence level). These last two regression analyses do use some of the same flux data that were used in constructing Fig. 4, but we believe that the three sets of flux indices are sufficiently independent to ensure the validity of the relationship between the pulse-width and flux spectral indices.

Accepting that the pulse-width and flux spectral indices are related, we find that the flatter width spectra are possessed by pulsars with the steeper flux spectra. It is indeed unfortunate that the two pulsars in Table 3 with the steeepest width spectra (0919+06 and 1842+14) do not have published fluxes above 0·4 GHz; the inclusion of their high-frequency flux spectra (which should be quite flat) could be decisive in establishing the suggested connection.

5. Discussion and Conclusions

We have combined our Culgoora measurements of pulse width at 80 and 160 MHz with most other published higher frequency widths. The resulting 24 pulse-width spectra have the following characteristics:

- (i) There is a basic power-law spectrum with index ranging between $+0\cdot 09$ and $-0\cdot 60$ with a median of $\beta = -0\cdot 16$.
- (ii) The spectrum of the spacings between the outer components of multiple profiles tends to have the same slope as that of the total width at $\nu < 1$ GHz, but flattens significantly at higher frequencies.
- (iii) The only statistically significant relationships between the pulse-width spectral index and intrinsic pulsar parameters are those involving the rate loss of rotational kinetic energy $\dot{E}$ and the high-frequency flux spectral index $\alpha^{\dagger}_{0\cdot 40}$. The former should be considered doubtful, while the latter appears to have a firmer basis.

The generally accepted polar emission model for pulsars has been proposed partly on the basis of the observed spectral behaviour of pulse width. This model proposes that the radio emission is produced in a hollow conical volume whose axis is coincident with the magnetic axis of the neutron star. The higher frequencies are generated nearer the apex of the cone, so that as the observer's line of sight sweeps across the cone a correspondingly narrow pulse will be seen. The variety of observed single to triple pulse profiles that can be reproduced by such a model was well illustrated and discussed by Backer (1976).

Our measurements of pulse-width spectral index are not however fully consistent with the $\nu^{-1/4}$ or $\nu^{-1/3}$ values predicted by Komesaroff (1970) and by Ruderman and Sutherland (1975) respectively. At the very least there must be significant departures from a dipole field to account for pulse-width spectral indices in the range $-0\cdot 6 < \beta < +0\cdot 1$.

Perhaps the most unexpected result of our study has been to establish a connection between the spectral width of the radio beam and the high-frequency flux spectral index. The existing theoretical computations based on the simple dipolar field model and the intensity of coherent curvature radiation (Komesaroff 1970) predict that the flux density will vary as ν^{-1}, while the profile width will vary as $\nu^{-0\cdot 25}$. Tademaru's (1971) analysis based on another model for the polar region gave the same frequency dependence for the pulse width. Tademaru also found that the spectral index for the emission by a thin sheet of radiating charges (thickness $<\lambda$) changes from $-0\cdot 5$ at low frequencies to -2 at high frequencies. The latter spectral slope is consistent with out median of $\alpha^{\dagger}_{0\cdot 40} = -1\cdot 9$ from Table 3, although there are clearly significant departures from this value. The observed median pulse-width spectral index of $\beta = -0\cdot 16$ is close to the suggested theoretical dependence, but again there are very significant departures which cannot be explained by the simple model; this is particularly true of the pulsars whose profiles actually increase in width with frequency. It is clear that the suggested α/β relationship, if confirmed by observations on more pulsars, provides a clue to the construction of more realistic models for pulsar emission.

Acknowledgments

We thank K. V. Sheridan for calibrating the CCA and G. W. Crapps and A. E. Spencer for designing and constructing the filter banks and square-law detectors. G. A. Dulk participated in the design of the CCA experiment and made some of the observations. R. N. Manchester kindly allowed us to use unpublished low-frequency profiles obtained at the Greenbank and Parkes observatories. A. G. Lyne and P. A. Hamilton supplied us with unpublished 1·42 GHz profiles from Jodrell Bank.

References

Alurkar, S. K., Slee, O. B., and Bobra, A. D. (1986). *Aust. J. Phys.* **39**, 433.
Ashworth, M., and Lyne, A. G. (1981). *Mon. Not. R. Astron. Soc.* **195**, 517.
Backer, D. C. (1970). *Nature* **228**, 1297.
Backer, D. C. (1972). *Astrophys. J.* **174**, L157.
Backer, D. C. (1976). *Astrophys. J.* **209**, 895.
Backer, D. C., Boriakoff, V., and Manchester, R. N. (1973). *Nature Phys. Sci.* **243**, 77.
Backer, D. C., and Fisher, J. R. (1974). *Astrophys. J.* **189**, 137.
Bartel, N., Kardashev, N. S., Kuzmin, A. D., Nikolaev, N. Ya., Popov, M. V., Sieber, W., Smirnova, T. V., Soglasnov, V. A., and Wielebinski, R. (1981). *Astron. Astrophys.* **93**, 85.
Craft, H. D., and Comella, J. M. (1968). *Nature* **220**, 676.
Crovisier, J. (1973). *Astrophys. Lett.* **13**, 221.

Gomez-Gonzales, J., Falgarone, E., Encrenaz, P., and Guelin, M. (1972). *Astrophys. Lett.* **12**, 207.

Guelin, M., Guibert, J., Huchtmeier, W., and Weliachew, L. (1969). *Nature* **221**, 249.

Hamilton, P. A., McCulloch, P. M., Ables, J. G., and Komesaroff, M. M. (1977). *Mon. Not. R. Astron. Soc.* **180**, 1.

Komesaroff, M. M. (1970). *Nature* **225**, 612.

Komesaroff, M. M., Morris, D., and Cooke, D. J. (1970). *Astrophys. Lett.* **5**, 37.

Krishna Mohan, S., Balasubramanian, V., and Swarup, G. (1971). *Nature Phys. Sci.* **234**, 151.

Kuzmin, A. D., Malofeev, V. M., Shitov, Yu. P., Davies, J. G., Lyne, A. G., and Rowson, B. (1978). *Mon. Not. R. Astron. Soc.* **185**, 441.

Lyne, A. G., Smith, F. G., and Graham, D. A. (1971). *Mon. Not. R. Astron. Soc.* **153**, 337.

McCulloch, P. M., Hamilton, P. A., Manchester, R. N., and Ables, J. G. (1978). *Mon. Not. R. Astron. Soc.* **183**, 645.

McLean, A. I. O. (1973). *Mon. Not. R. Astron. Soc.* **165**, 133.

Manchester, R. N. (1971). *Astrophys. J. Suppl. Ser.* **23**, 283.

Manchester, R. N. (1975). *Proc. Astron. Soc. Aust.* **2**, 334.

Manchester, R. N., Hamilton, P. A., and McCulloch, P. M. (1980). *Mon. Not. R. Astron. Soc.* **192**, 153.

Manchester, R. N., Lyne, A. G., Taylor, J. H., Durdin, J. M., Large, M. I., and Little, A. G. (1978). *Mon. Not. R. Astron. Soc.* **185**, 409.

Manchester, R. N., and Taylor, J. H. (1981). *Astron. J.* **86**, 1953.

Morris, D., Graham, D. A., Sieber, W., Bartel, N., and Thomasson, P. (1981). *Astron. Astrophys. Suppl. Ser.* **46**, 421.

Morris, D., Schwarz, U. J., and Cooke, D. J. (1970). *Astrophys. Lett.* **5**, 181.

Rankin, J. M. (1983). *Astrophys. J.* **274**, 333.

Rankin, J. M., and Benson, J. M. (1981). *Astron. J.* **86**, 418.

Ruderman, M. A., and Sutherland, P. G. (1975). *Astrophys. J.* **196**, 51.

Schönhardt, R. E., and Sieber, W. (1973). *Astrophys. Lett.* **14**, 61.

Schwarz, U. J., and Morris, D. (1971). *Astrophys. Lett.* **7**, 185.

Sieber, W., Reinecke, R., and Wielebinski, R. (1975). *Astron. Astrophys.* **38**, 169.

Sieber, W., and Wielebinski, R. (1973). *Astrophys. Lett.* **13**, 225.

Slee, O. B., Alurkar, S. K., and Bobra, A. D. (1986). *Aust. J. Phys.* **39**, 103.

Tademaru, E. (1971). *Astrophys. Space Sci.* **12**, 193.

Manuscript received 24 November 1986, accepted 23 February 1987